



Ultraviolet B modulates gamma radiation-induced stress responses in *Lemna minor* at multiple levels of biological organisation



Li Xie^{a,c,*}, You Song^{a,c}, Karina Petersen^a, Knut Asbjørn Solhaug^{b,c}, Ole Christian Lind^{b,c}, Dag Anders Brede^{b,c}, Brit Salbu^{b,c}, Knut Erik Tollefsen^{a,b,c,*}

^a Norwegian Institute for Water Research (NIVA), Section of Ecotoxicology and Risk Assessment, Økernveien 94, N-0349 Oslo, Norway

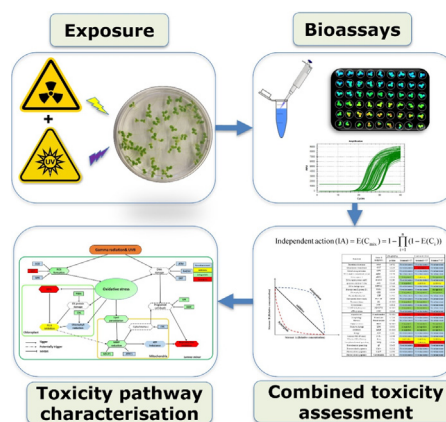
^b Norwegian University of Life Sciences (NMBU), Faculty of Environmental Sciences and Natural Resource Management (MINA), N-1432 Ås, Norway

^c Norwegian University of Life Sciences (NMBU), Centre for Environmental Radioactivity, N-1432 Ås, Norway

HIGHLIGHTS

- Mechanistic-informed combined toxicity assessment for ionizing and non-ionizing radiation demonstrated in *Lemna minor*.
- Additivity and antagonism were observed at subcellular and cellular levels, while synergism occurred at the population level.
- Target- and dose rate-specific combined effects were characterised by a toxicity pathway network model.

GRAPHICAL ABSTRACT



ARTICLE INFO

Editor: Daniel Wunderlin

Keywords:

Multiple stressors
Ionizing radiation
Solar radiation
Aquatic macrophyte
Combined effect modelling
Toxicity pathway

ABSTRACT

Elevated levels of ionizing and non-ionizing radiation may co-occur and pose cumulative hazards to biota. However, the combined effects and underlying toxicity mechanisms of different types of radiation in aquatic plants remain poorly understood. The present study aims to demonstrate how different combined toxicity prediction approaches can collectively characterise how chronic (7 days) exposure to ultraviolet B (UVB) radiation (0.5 W m^{-2}) modulates gamma (γ) radiation ($14.9, 19.5, 43.6 \text{ mGy h}^{-1}$) induced stress responses in the macrophyte *Lemna minor*. A suite of bioassays was applied to quantify stress responses at multiple levels of biological organisation. The combined effects (no-enhancement, additivity, synergism, antagonism) were determined by two-way analysis of variance (2 W-ANOVA) and a modified Independent Action (IA) model. The toxicological responses and the potential causality between stressors were further visualised by a network of toxicity pathways. The results showed that γ -radiation or UVB alone induced oxidative stress and programmed cell death (PCD) as well as impaired oxidative phosphorylation (OXPHOS) and photosystem II (PSII) activity in *L. minor*. γ -radiation also activated antioxidant responses, DNA damage repair and chlorophyll metabolism, and inhibited growth at higher dose rates ($\geq 20 \text{ mGy h}^{-1}$). When co-exposed, UVB predominantly caused non-interaction (no-enhancement or additive) effects on γ -radiation-induced antioxidant gene expression, energy quenching in PSII and growth for all dose rates, whereas antagonistic effects were observed for lipid peroxidation, OXPHOS, PCD, oxidative stress, chlorophyll metabolism and genes involved in DNA damage responses. Synergistic effects were observed for changes in photochemical quenching and non-photochemical quenching, and up-regulation of

* Corresponding authors at: Norwegian Institute for Water Research (NIVA), Section of Ecotoxicology and Risk Assessment, Økernveien 94, N-0349 Oslo, Norway.
E-mail addresses: lix@niva.no (L. Xie), kett@niva.no (K.E. Tollefsen).

antioxidant enzyme genes (*GST*) at one or more dose rates, while synergistic reproductive inhibition occurred at all three γ -radiation dose rates. The present study provides mechanistic knowledge, quantitative understanding and novel analytical strategies to decipher combined effects across levels of biological organisation, which should facilitate future cumulative hazard assessments of multiple stressors.

1. Introduction

In the aquatic environment, organisms are exposed to background radiations, including ionizing radiation and non-ionizing radiation. Ionizing radiation, such as gamma (γ) radiation, are generated from natural sources (e.g., naturally occurring radioactive material, and cosmic radiation) and anthropogenic sources such as nuclear weapons tests, nuclear accidents and uranium mining (UNSCEAR, 2021). Elevated background levels of γ -radiation due to the increase of authorised discharges or accidental releases of radioactive material could pose a serious threat to ecosystems. Non-ionizing radiation, such as ultraviolet B (UVB), is a key part of the solar radiation at the earth's surface, and varies with time, latitude, altitude, solar zenith angle, and cloud cover (Lubin et al., 1998). As an essential environmental factor, UVB is known to play a critical role in the ecosystem (Bornman et al., 2019). In radioactively contaminated areas, biota can be directly exposed to elevated levels of γ -radiation as well as to UVB that collectively cause combined toxicity that are not predicted on basis of the effects of single stressors alone. Such multiple stressor effects are often not addressed and seldomly quantitated (Salbu et al., 2019), making studies to address joint toxicity of non-chemical stressors highly relevant.

In the aquatic ecosystem, primary producers are important energy and nutrition sources at the base of the food chains. Among them, macrophytes are frequently found living in slow or still flowing water habitats, thus facing exposure to γ -radiation from contaminated catchments. It has been reported that γ -radiation associated with contaminated surface waters ranges from 0.1 to $1 \times 10^3 \mu\text{Gy h}^{-1}$ (Cochran et al., 1993; Kryshev et al., 1997), while the worldwide average dose rate of background ionizing radiation is estimated to be around $0.27 \mu\text{Gy h}^{-1}$ (Thorne, 2003). In extreme cases such as in Lake Karachay in Mayak, the estimated absorbed dose rate of ionizing radiation for phytoplankton exceeded $1.7 \times 10^6 \mu\text{Gy h}^{-1}$ in 2012 (Shuryak, 2018). Exposure to elevated levels of γ -radiation is known to generate reactive oxygen (ROS) and nitrogen (RNS) species in primary producers, thereby causing oxidative damage to macromolecules (DNA, proteins and lipids) as well as direct radiation-induced DNA double-strand breaks (DSB) (Caplin and Willey, 2018). Adverse effects of γ -radiation have been investigated in detail in terrestrial plants, such as *Glycine max* (Alikamanoglu et al., 2011), *Arabidopsis thaliana* (Vanhoudt et al., 2014), and *Oryza sativa* (Jan et al., 2012), and aquatic plant such as *Lemna minor* (Xie et al., 2019).

Compared to γ -radiation, the impact of UVB radiation is well documented in primary producers due to the Ozone depletion in the past few decades. Despite improvements with respect to ozone depletion and partial recovery of stratospheric ozone, impacts of UVB on organisms are still a matter of concern (Bernhard et al., 2020). Currently, the average background irradiance of UVB ranges from 0.23 to 1.55 W m^{-2} during summer in western and northern Europe (Jablonski and Chaplin, 2010; Johnsen, 2022), which can be harmful to primary producers that are poorly acclimated or subjected to exposure for prolonged periods of time (Hollosy, 2002; Czegeny et al., 2016; Fraikin, 2018b). UVB is capable of causing DNA lesions by inducing photoproducts such as cyclobutane pyrimidine dimers (CPD) and pyrimidine (6–4) pyrimidone dimers (Hidema et al., 2007). Exposure to UVB is also known to disrupt redox reaction-based physiological processes and produce excessive ROS in organisms (Hideg and Vass, 1996). Additionally, the photosynthetic apparatus has also been reported to be the initial target of UVB, which directly regulates the growth of plants (Teramura and Sullivan, 1994). UVB-induced DNA damage, oxidative stress, and inhibition of photosynthesis and growth have been well studied in different plants such as *A. thaliana*, *Vicia faba*, *G. max* and *L. minor* (Teramura and Sullivan, 1994; Vu et al., 1981; Xie et al., 2020). In

addition, UVB also plays a regulatory role in plants by modulating key physiological processes such as auxin and gibberellin production,

So far, however, investigations of the combined effects of these radiations are seldomly addressed in aquatic primary producers. Furthermore, despite a number of studies reporting combined effects of various environmental stressors on aquatic plants, the majority of available studies focuses on apical or molecular endpoints, without providing a holistic picture of how combined effects at different levels of biological organisation. The lack of systemic and mechanistic understanding of key events in these toxicity pathways may thus limit our ability to quantitate and characterise how combined toxicity occur. To assess the combined effects of environmental stressors, two classical models originally developed for assessing chemical mixture toxicity are often used. The concentration addition (CA) model assumes a common biological target and mode of action (MoA) of the stressors (Rozema et al., 1997), whereas the independent action (IA) model assumes dissimilar targets and MoAs of the stressors (Bliss, 1939). Stressors affecting the same endpoint are suitable for combined assessments according to the traditional CA models. Both models assume additive effects of the stressors, whereas deviations from model predictions are either synergistic (more than additive) when observed effects are larger than predictions, or antagonistic when observations are less severe than predictions. The IA model predicts the combined effects based on the joint probability of the effects occurring by independent stressors (Bliss, 1939), while the CA models typically require well developed dose-response curves (DRC). Therefore, the concept of IA can be used in simpler experimental designs (Jonker et al., 2005) and several modified versions have addressed joint effects at the molecular as well as organism level (Song et al., 2018; Bradshaw et al., 2019). More extensive implementation of modified IA models for assessing the combined effects of different types of stressors (chemical and non-chemical) could be beneficial as effects of multiple stressors are typically characterised by different MoAs.

The present study was conducted to conceptually demonstrate how joint effects of γ -radiation and UVB on aquatic plants can be characterised using a combination of different combined toxicity prediction models. The overall objective of the present work was to implement a modified IA model for assessing the combined effects of γ -radiation and UVB. Although additivity is commonly assumed to occur between chemical stressors, interaction giving rise to either antagonism or synergism seems more relevant for co-exposures to multiple stressors including ionizing radiation (Salbu et al., 2019). Therefore, it is hypothesised that exposure to the combination of γ -radiation and UVB radiation would cause more than additive effects in plants at different levels of biological organisations, ranging from molecular responses to more apical adverse effects. In the present work, common duckweed *Lemna minor* was used as a model macrophyte, due to the advantages of small size, rapid life cycles, easy cultivation, high sensitivity and standardised testing protocols (Radić et al., 2010). In brief, *L. minor* was exposed to a single irradiance of UVB, three dose rates of γ -radiation, and their combinations for 7 days to assess the toxic responses at multiple levels of biological organisation (e.g. responses at the molecular, cellular, tissue, organ, and individual level). The combined effects of the stressors were evaluated using a combination of two-way analysis of variance (2 W-ANOVA) and a modified IA model. The results were assembled into a set of conceptual toxicity pathways to visualise potential interactions giving rise to the observed toxicity.

2. Materials and methods

2.1. *Lemna* culture

Lemna minor (strain ID: 5544, Rutgers Duckweed stock cooperative) was originally obtained from Ghent University, Belgium. Fronds were

cultured in Swedish Standard (SIS medium) culture medium as detailed in Xie et al. (2019). All cultures were maintained in a growth chamber with incandescent light in photosynthetic active radiation (PAR) at $80 \pm 5 \mu\text{mol m}^{-2} \text{s}^{-1}$ in a 16 h light/8 h dark photoperiod and temperature of $22 \pm 2 \text{ }^\circ\text{C}$, with stock thalli sub-cultured twice a week. The PAR was measured by an LI-COR quantum sensor Model LI-190 (Lincoln, Nebraska, USA) connected to an LI-COR LI-250 photometer unit.

2.2. Exposure

The exposure was performed in the climate chambers at the FIGARO experimental facility at the Norwegian University of Life Sciences (NMBU, Ås, Norway) equipped with a ^{60}Co (1173.2 and 1332.5 keV γ -rays) γ -radiation source (Lind et al., 2019). Prior to exposure, *L. minor* was acclimatised in the exposure chambers for 14 days with SIS medium and the same culture conditions as described above in Section 2.1. Only healthy *L. minor* colonies with green fronds were used. For the radiation exposure, Petri dishes (60 mm \times 15 mm, Nunc™, Oslo, Norway) with 30 ml SIS medium and 6 fronds (2 colonies) in each well ($N = 6$) were positioned at different distances away from the γ -source to obtain specific gamma dose-rates to water (D_{Water}) inside the climate (UVB irradiance) chambers (Fig. 1). The gamma dosimetry of the exposed plants followed the established protocol detailed by Hansen et al. (2019). The Petri dishes were rotated 180° every 24 h to give all wells the same dose rates and total doses. Dose rates to water in the centre of the petri dish were estimated according to Bjerke and Hetland (2014) and used as a proxy for the dose rates to *L. minor*. Actual gamma dose rates were measured by an Optically Stimulated Luminescence (OSL) based dosimetry system using nanoDots dosimeters and an InLight microSTAR reader (Landauer®, Velizy-Villacoublay Cedex, France). Nanodots with 5 mm polypropylene build-up caps were exposed in front of, and at the back of the Petri dishes to determine the average dose rates (mGy h^{-1}), the dose rate ranges within the Petri dishes (mGy h^{-1}) and the total doses (Gy) after 7 days of exposure (Table 1).

The UVB radiation in each climate chamber was provided by 4 UVB fluorescent tubes (UVB-313, Q-Panel, Cleveland, USA) and plants exposed for 16 h light per day in the climate chamber at Figaro. Cellulose diacetate foil (0.13 mm, Jürgen Rachow, Hamburg, Germany) was placed on top of the microplates to block UV wavelengths below 290 nm for UVB treatment (UV+) groups, while the non-UVB treatment (UV-) groups were covered with pre-burned (24 h exposed to 1 W m^{-2} UVB) polyester foil (0.175 mm, Nordbergs Tekniska AB, Vallentuna Sweden) to completely block

Table 1

Dose rates (mGy h^{-1}) and total doses (Gy) used in the gamma radiation exposures of *Lemna minor* for 168.5 h using the FIGARO ^{60}Co source.

Average Dose rate (mGy h^{-1})	Dose rate interval (mGy h^{-1})		Average Total dose (Gy)	Total dose interval (Gy)	
	Minimum	Maximum		Minimum	Maximum
43.6	42.3	44.8	7.4	7.1	7.6
19.5	18.6	19.5	3.3	3.1	3.4
14.9	14.3	15.4	2.5	2.4	2.6
0.005 ^a	0.004	0.006	0.84	1.008	0.672

^a Dose rate of control in the Lead-shielded control zone.

UVB and most of the UVB radiation (wavelength $< 315 \text{ nm}$). The UVB irradiance was measured with a broadband UVB sensor (SKU340, Skye Instruments, Powys, UK). The transmittance spectrum of polyester and cellulose acetate filters was detailed in Xie et al. (2020), and confirmed that these filters did not impact the spectrum of PAR. Based on calibration factors from simultaneous measurement of UVB with an Optronic model 756 spectroradiometer (Optronic laboratories, Orlando, FL, USA), the absolute UVB irradiation was calculated to be $0.49 \pm 0.01 \text{ W m}^{-2}$ (total effective dose $197.6 \pm 4 \text{ kJ m}^{-2}$).

2.3. Growth inhibition

After exposure for 7 days, the growth rate parameters, including frond number, frond size and fresh weight, were measured essentially as described by Xie et al. (2019). Frond number (FN) was recorded before and after the exposure to calculate the reproductive inhibition as described in the OECD 221 Test guideline "*Lemna sp.* Growth Inhibition Test" (OECD, 2006). The frond area was measured on basis of the whole-plant imaging by a digital camera (FinePix S2500HD, Fujifilm, Japan) with engineering graph paper in standard imperial/US and metric scales. The frond area in each photograph was analysed using the software Image-J version 1.48 (National Institutes of Health, Maryland, USA). The fresh weight was measured by weighing all material, including fronds and roots from one well after drying off excessive fluid by a dry lint-free paper tissue. Results were presented as fold change compared to blank control (without γ -radiation and UVB).

2.4. ROS assay

Cellular ROS formation was quantified using the 2',7'-Dichlorofluorescein diacetate (H_2DCFDA) assay (Molecular Probes Inc., Eugene, OR, USA), as described by Xie et al. (2019). Briefly, a 50 mM H_2DCFDA stock solution was prepared in dimethyl sulfoxide (DMSO) (Purity 99.7 %; Sigma-Aldrich, St-Louis, USA) and stored at $-20 \text{ }^\circ\text{C}$ until use. Fronds were immersed in 200 μL working solution of H_2DCFDA (50 μM) prepared in the culture medium after the exposure. After 1 h probe loading, the fronds were rinsed with a clean medium and transferred to a black 96-well microplate (Corning Incorporated, Costar®, NY, USA). The fronds were immediately measured using a VICTOR³ fluorescent plate reader, 1400 Multilabel Counter (Perkin Elmer, Massachusetts, USA) with excitation/emission wavelengths of 485/538 nm. Results were presented as fold change compared to control. The raw fluorescent counts were normalised by the weight of the fronds and were presented as fold changes compared to the blank control.

2.5. TBARS assay

Lipid peroxidation (LPO) was measured by analysing the content of Malondialdehyde (MDA), a marker of LPO as described by Radić et al. (2010), with minor modifications (Xie et al., 2018). In general, 12 fronds were homogenised in 1 ml of 0.25 % (w/v) 2-thiobarbituric acid (TBA, Sigma-Aldrich) in 10 % trichloroacetic acid (TCA, Sigma-Aldrich) and incubated at $95 \text{ }^\circ\text{C}$ for 30 min. After incubation, the fronds were cooled in

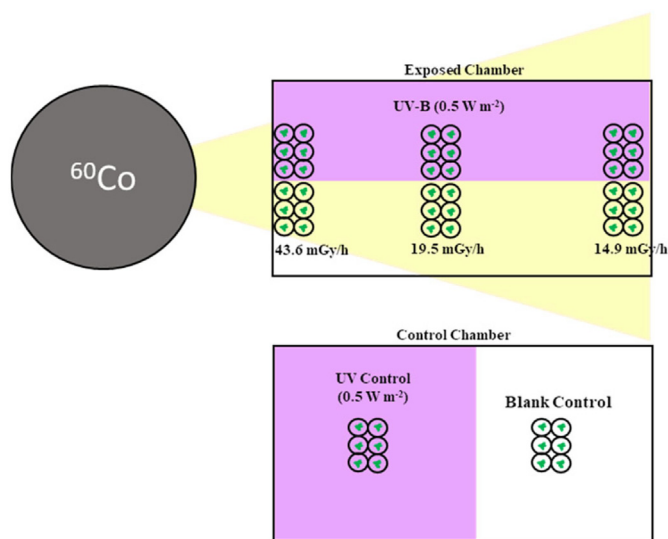


Fig. 1. Schematic diagram of combined exposure of γ -radiation and UVB radiation. The yellow area represented the gamma radiation beam emitted from a cobalt-60 (^{60}Co) source, while the purple represented the area exposed to UVB. The γ -radiation dose rate was adjusted by changing the distance to the ^{60}Co source.

an ice bath for 10 min and centrifuged at $10,000 \times g$ for 10 min ($< 4^\circ\text{C}$). The absorbance of the supernatant was measured at 532 nm and corrected for non-specific turbidity by subtracting the absorbance at 600 nm. A background control containing 0.25 % TBA in 10 % TCA was also analysed and subtracted from the total absorbance in the samples. The MDA level was presented as $\mu\text{mol g}^{-1}$ using an extinction coefficient of $155 \text{ nmol}^{-1} \text{ cm}^{-1}$ (Hashem, 2013). Results were presented as fold change compared to blank control.

2.6. TMRM assay

As a proxy for mitochondrial oxidative phosphorylation, mitochondrial inner membrane potential (MMP) was characterised using tetramethylrhodamine methyl ester (TMRM, Invitrogen Molecular Probe, Eugene, Oregon, USA). In brief, stock solutions of TMRM (5 mM) were prepared in DMSO and stored at -20°C until use. $2 \mu\text{L}$ TMRM stock solution was added into SIS medium to make a 500 nM working solution immediately prior to staining. One *L. minor* colony with 3 fronds were transferred into the well at the end of the exposure. The fronds were then incubated with 200 μL TMRM working solution in the dark (1 h, room temperature), rinsed with SIS medium for 5 min to remove free (unbound) TMRM and transferred to 200 μL SIS medium in 96-well black clear-bottom microplate. The fluorescent intensity of internally incorporated TMRM was measured using VICTOR³, 1400 Multilabel Counter using the excitation wavelength of 530 nm and the emission wavelength of 590 nm. Results were presented as fold change compared to blank control (without γ -radiation and UVB).

2.7. Photosystem II performance

Performance of the photosystem II (PSII) was characterised simultaneously for all samples by a pulse-Amplitude-Modulated (PAM) chlorophyll fluorescence kinetics using a PAM 2000 fluorometer (Walz, Effeltrich, Germany). After being dark-adapted for 30 min, the basal fluorescence (F_o) was measured under weak modulated illumination ($1 \mu\text{mol m}^{-2} \text{ s}^{-1}$), and the maximum fluorescence (F_m) was obtained by applying a saturating light pulse ($5000 \mu\text{mol m}^{-2} \text{ s}^{-1}$, 0.8 s). The light-adapted fluorescence parameters such as effective minimal fluorescence (F_o') and steady-state terminal fluorescence (F) were measured in the state of open photosystem II reaction centres after 30 min of continuous illumination of $80 \mu\text{mol m}^{-2} \text{ s}^{-1}$ from a high-intensity LED panel (Model SL-3500, Photon System Instruments, Brno, Czech Republic). The F_o' was measured in the presence of far-red illumination with the Actinic Light source switched off, while the value of F_t was measured shortly before a light Saturation Pulse. Light adapted maximal fluorescence (F_m') was obtained by applying a saturating light pulse. The values determined during the measurement (F_o , F_o' , F_m , F_m' and F) allowed the calculation of the maximum quantum yield of the photosystem (F_v/fm) and operating efficiency of PSII ($\Phi_{\text{PSII}} = (F_m' - F)/f_m'$). The photochemical parameters such as non-photochemical quenching (NPQ) and photochemical quenching (qP) were calculated using the equations ($\text{NPQ} = (F_m - F_m')/f_m'$ and $qP = (F_m' - F)/(F_m - F_o')$) as described by (Baker, 2008). The results were presented as percentage inhibition compared to blank control.

2.8. Pigment measurement

Pigment content was measured spectrophotometrically, essentially as described by Lichtenthaler (1987). After exposure, 25 mg of whole plant tissue (wet weight) including fronds and roots were homogenised in 2 ml methanol (99.9 %, Sigma-Aldrich, Oslo, Norway) in darkness at 4°C overnight to avoid degradation, then centrifuged at 3000 rpm for 10 min. The absorbance of the supernatant at 652, 665 and 470 nm was determined by a UV/VIS spectrophotometer (Perkin-Elmer, Lambda 40, Akron, Ohio, USA) as detailed in Xie et al. (2018). The contents of chlorophylls (chlorophyll *a* and *b*) and total carotenoids were calculated as described by Nayek et al. (2014). Results were presented as percentage inhibition compared to blank control after normalisation to wet weight.

2.9. ATP assay

ATP content in the *L. minor* fronds was quantified by Luminescence ATP Detection Assay Kit (ab113849, Abcam, UK) with some modification. Briefly, 3 fronds from each treatment were homogenised in 100 μL PBS and transferred into 96 black microplates where 50 μL detergent (supplied by kit) was added. The plate was shaken/vortexed gently, and 50 μL Substrate Solution was added prior to shaking for an additional 5 min as described in the manufacturer's instructions. The luminescence was measured by a Wallac Microbeta Jet 1450 microplate Scintillation/Luminescence counter (PerkinElmer Life Sciences, Gaithersburg, MD) after 10 min dark adaptation. Results were presented as percentage inhibition compared to the blank control after normalisation to wet weight.

2.10. Transcription analysis

After exposure for 7 days, 6 fronds from each petri dish were snap-frozen in liquid nitrogen and stored at -80°C until use. Quick-RNA Plant RNA MiniPrep kit (Zymo Research Corp., Irvine, CA) was used for total RNA extraction according to the manufacturer's protocols. Purity and integrity of RNA ($260/230 \geq 1.8$, $260/280 \geq 1.8$, $\text{RIN} \geq 6.0$) were assessed using a Nanodrop ND-1000 (Nanodrop Technologies, Wilmington, DE) and a Bioanalyzer (Agilent Technologies, Santa Clara, CA, USA), respectively. The quantitative real-time reverse transcription-polymerase chain reaction (qPCR) assay was performed as previously described (Song et al., 2016). In brief, each RNA sample (100 ng) was reverse-transcribed into cDNA using qScriptTM cDNA SuperMix (Quanta BioSciencesTM, Gaithersburg, MD, USA). The design of primers was performed using Primer 3 v0.4.0 (<http://bioinfo.ut.ee/primer3-0.4.0/>) and purchased from InvitrogenTM (Carlsbad, California, USA). All primer sequences and relevant information are presented in Supplementary Table S1. The qPCR was performed in a CFX384 Real-Time PCR Detection System (Bio-Rad Laboratories, Philadelphia, PA, USA). Each reaction mixture consisted of 1 μL of cDNA template, 15 μL of PerfeCTa[®] SYBR[®] Green FastMix[®] (Quanta BioSciencesTM) and 400 nM of forward/reverse primer in a total volume of 20 μL . Pooled cDNA (0.25–4 ng) from all samples were used to generate the standard curve for calculation of amplification efficiency ϵ and correlation coefficient. No-reverse-transcriptase control (NRT) and no-template control (NTC) were also included in amplification for quality controls. The relative expression was calculated using the Pfaffl method (Pfaffl, 2001), and normalised to the geometric mean expression of reference genes, glyceraldehyde 3-phosphate dehydrogenase (*Gadph*), 40s ribosomal protein S18 (Pfaffl, 2001), and elongation factor 1- α (*Ef1a*) (Shi et al., 2016; Tang et al., 2017) according to the $\Delta\Delta\text{C}_q$ method (Vandesompele et al., 2002).

2.11. Combined effect assessment

The combined effects of γ -radiation and UVB were assessed by a combination of two-way (2 W) ANOVA and a modified IA model originally proposed by Jonker et al. (2005) and modified to address molecular response data by Song et al. (2018). In detail, experimental data from single and combined exposures were subjected to a two-way analysis of variance (2 W-ANOVA) to determine whether the stressors displayed similar effect patterns, whether biological interactions occurred for the stressors or whether no interactions (no-enhancement or additivity) were occurring. In combination with the 2 W-ANOVA, a modified IA model was used to assess whether the observed combined response agreed with, or deviated from, the assumption of additivity. In brief, the predicted combined effect ($M_{\text{pre(combined)}}$) was calculated using the following equations, as previously described by Song et al. (2018):

$$M_{\text{pre(combined)}} = \text{Log}2\left(\frac{Y_{\text{obs(Gamma)}}}{Y_{\text{obs(Ctrl)}}}\right) + \text{Log}2\left(\frac{Y_{\text{obs(UV)}}}{Y_{\text{obs(Ctrl)}}}\right) \quad (1)$$

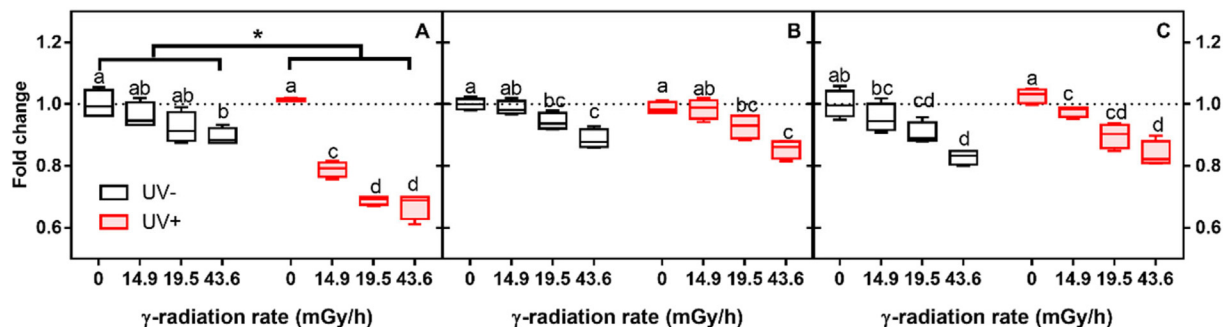


Fig. 2. Effect of gamma radiation on the growth of *Lemna minor* after exposure with (UV+) or without UVB (UV-) for 7 days: (A) fronds number, (B) frond size and (C) fronds weight. Boxes represent the median ($N = 6$) and the 25th and 75th percentiles, and the whiskers represent the minimum and maximum value. The dotted line indicates the base level of responses in the control group. Different letters indicate significant differences in means between treatments, while the asterisk “*” denotes significant interaction between groups with or without UVB ($p \leq 0.05$).

where the $Y_{obs(Gamma)}$ is the observed effect after exposure to γ -radiation, $Y_{obs(UV)}$ is the observed effect after exposure to UVB, and $Y_{obs(Ctrl)}$ is the observed effect from control.

The observed combined effect ($M_{obs(combined)}$) was calculated by the equation:

$$(M_{obs(combined)}) = \text{Log2} \left(\frac{Y_{obs(combined)}}{Y_{obs(Ctrl)}} \right) \quad (2)$$

where $Y_{obs(combined)}$ is the observed effect after the combined exposure of γ -radiation and UVB.

The combined effects of the two stressors were quantitatively assessed based on the overlapping between predicted ($M_{pre(combined)} \pm CI_{pre}$) and observed data ($M_{obs(combined)} \pm CI_{obs}$), where the CI is the 95 % confidence interval of deviation:

$$\text{Additivity or no - enhancement} : M_{obs(combined)} \pm CI_{obs} \cap M_{pre(combined)} \pm CI_{pre} \neq \emptyset \quad (3)$$

No enhancement was defined as the incidents where no interactions between γ -radiation and UVB and UVB did not cause any significant effects alone. In contrast, additive effects were defined when UVB caused significant effects but did not modulate the effects of γ -radiation beyond exposure to γ -radiation alone.

$$\text{Synergism} : M_{obs(combined)} \pm CI_{obs} > M_{pre(combined)} \pm CI_{pre} \quad (4)$$

$$\text{Antagonism} : M_{obs(combined)} \pm CI_{obs} < M_{pre(combined)} \pm CI_{pre} \quad (5)$$

2.12. Statistics

All statistical analyses were performed using GraphPad Prism version 6 (GraphPad Software, California, USA). The results for each endpoint were presented as boxplots. Data were assessed for normality and homogeneity of variance by the Shapiro-Wilk and Levene's tests, respectively. Statistical analysis was additionally performed by a 2 W-ANOVA to identify interactions between stressors. A Dunnett's multiple comparison test using a significance level of $p \leq 0.05$ were used to identify significant differences between individual exposure groups.

3. Results

3.1. Growth rate

The average fronds reproduction rate of *L. minor* in the non-UV control was 0.421 d^{-1} and was above the validity limit for the OECD 221 test guideline (average specific growth rate of 0.275 d^{-1} ; OECD, 2006).

Gamma exposure alone caused a dose rate-dependent reduction in all three growth endpoints in *L. minor* (Fig. 2), albeit significant growth inhibition was only observed at the highest gamma dose rate (43.6 mGy h^{-1}). Up to 20 % reduction of frond weight (FW) was observed at 43.6 mGy h^{-1} , whereas frond number (FN) and frond size (FS) were reduced by 10 % and 12 % at the same dose rate, respectively. However, the UVB exposure did not cause any significant effects on the growth parameters of *L. minor*. In the combined exposures, the 2 W-ANOVA demonstrated a significant interaction between the two radiations in terms of FN (see Table 2 for details), whereas no-interactions were observed for the reduction of FS and FW. The IA modelling and CI overlapping test revealed that the synergistic interaction with respect to FN reduction was significant, and no enhancement in FS and FW was observed (Table 2).

3.2. Oxidative stress and damage

The results demonstrated that both γ -radiation and UVB individually enhanced the cellular ROS level and LPO in *L. minor*. When fronds were exposed to elevated γ -radiation, cellular ROS increased in a dose rate dependent manner to a maximum of 1.4-fold at 43.6 mGy h^{-1} . Maximum induction of LPO (1.3-fold) was also observed at the same dose rate (Fig. 3.A). Single UVB exposure caused a significant increase in ROS (1.4-fold) and LPO (1.5-fold) compared to control. In the combined exposures, significant interactions were detected by 2 W-ANOVA for ROS and LPO, and the IA modelling and CI overlapping test identified these interactions caused antagonism for ROS and LPO (Table 2).

3.3. Oxidative phosphorylation (OXPHOS) and ATP content

Exposure to γ -radiation alone caused a dose rate dependent reduction of MMP (OXPHOS) in *L. minor*, with a maximum reduction of MMP (0.8-fold) at 43.6 mGy h^{-1} (Fig. 4). However, no significant change in total ATP content in *L. minor* was observed for the single γ -radiation exposure. Exposure to UVB alone significantly inhibited MMP by 25 % at 0.5 W m^{-2} . In the combined exposure, the results of the 2 W-ANOVA identified that the two stressors were interacting in terms of inducing MMP reduction, and the combination of the IA prediction and CI overlapping test demonstrated that these interactions were antagonistic (Table 2). The 2 W-ANOVA and IA modelling demonstrated that no significant interaction and no-enhancement by the two stressors were observed on ATP content when exposed in combination (Table 2).

3.4. PSII performance

When exposed alone, γ -induced impacts on PSII parameters were observed with a maximum reduction of Φ_{PSII} (0.85-fold) and NPQ (0.8-fold) at 43.6 mGy h^{-1} , while no significant change was observed for F_v/fm and qP at any dose rate (Fig. 5). Exposure to UVB alone caused significant

Table 2

Summary of combined effects of γ -radiation and UVB in *Lemna minor* after 7 days co-exposure. Interactions was determined by 2 W-ANOVA (significant: $p \leq 0.05$), while the combined effects were evaluated by independent action (IA) model. Gamma 10 = 14.9 mGy h⁻¹ γ -radiation, Gamma 20 = 19.5 mGy h⁻¹ γ -radiation, Gamma 40 = 43.6 mGy h⁻¹ γ -radiation; UVB = 0.49 W m⁻² UVB. Observation and IA model prediction results are listed in Supp. Table S2.

Function	Biological organisation	Target	Target abbreviation	2W-ANOVA	IA model assessment*		
				p-value	Gamma 10+UVB	Gamma 20+UVB	Gamma 40+UVB
Oxidative stress and lipid peroxidation	Gene	Superoxide dismutase	<i>SOD</i>	0.670-1	Blue	Blue	Blue
	Gene	Glutathione s-transferase	<i>GST</i>	0.0209	Blue	Red	Blue
	Gene	Glutathione peroxidase	<i>GPX</i>	0.0524	Blue	Blue	Blue
	Gene	Flavonoid production	<i>CYP</i>	0.1421	Blue	Blue	Blue
	Molecular	ROS formation	<i>ROS</i>	<0.0001	Green	Green	Green
	Cellular	Malondialdehyde	<i>MDA</i>	0.0002	Green	Green	Green
DNA damage and programmed cell death	Gene	DNA double-strand break sensor	<i>ATM</i>	0.0596	Blue	Blue	Blue
	Gene	DNA repair protein rad50	<i>RAD50</i>	0.-1-161	Blue	Blue	Blue
	Gene	DNA-damage repair/tolerant protein 111	<i>DRT111</i>	0.76-14	Blue	Blue	Blue
	Gene	Metacaspase-1	<i>AMCI</i>	0.0058	Green	Yellow	Green
	Gene	Apoptosis inhibitor 5-like	<i>API5</i>	0.0446	Green	Yellow	Yellow
Photosynthesis	Gene	Photosystem II protein D1	<i>PSBA</i>	0.0054	Blue	Blue	Green
	Gene	Chlorophyllase	<i>CLH</i>	0.00-12	Green	Green	Green
	Gene	Carotenoids biosynthesis	<i>PSY75B</i>	0.6559	Blue	Blue	Blue
	Subcellular	Maximal PSII efficiency	F_v/F_m	0.0549	Blue	Blue	Blue
	Subcellular	Effective PSII efficiency	Φ_{PSII}	0.958	Yellow	Yellow	Yellow
	Subcellular	Non-photochemical quenching	<i>NPQ</i>	0.0006	Red	Yellow	Red
	Subcellular	Photochemical quenching	<i>qP</i>	0.0405	Blue	Red	Blue
	Subcellular	Chlorophyll <i>a</i>	<i>Chl a</i>	0.1118	Blue	Blue	Blue
	Subcellular	Chlorophyll <i>b</i>	<i>Chl b</i>	0.2642	Blue	Blue	Blue
	Subcellular	Total carotenoids	<i>Car</i>	0.0765	Blue	Blue	Blue
Glycolysis and oxidative phosphorylation	Gene	Pyruvate kinase	<i>PK</i>	<0.0001	Green	Green	Blue
	Gene	Cytochrome c	<i>CYC</i>	0.0918	Blue	Blue	Blue
	Gene	NADH dehydrogenase	<i>NDUFVI</i>	<0.0001	Green	Green	Blue
	Gene	ATP synthase	<i>ATPC</i>	0.-1148	Blue	Blue	Blue
	Subcellular	OXPHOS	<i>MMP</i>	<0.0001	Green	Green	Green
	Cellular	ATP content	<i>ATP</i>	0.286	Blue	Blue	Blue
Growth and reproduction	Individual	Fronde size	<i>FS</i>	0.7526	Blue	Blue	Blue
	Individual	Fronde weight	<i>FW</i>	0.7488	Blue	Blue	Blue
	Population	Fronde number	<i>FN</i>	<0.0001	Red	Red	Red

*Combined effects determined as no-enhancement (blue), antagonism (green), additivity (yellow) and synergism (red).

inhibition of Φ_{PSII} (0.9-fold), but no statistically significant effects on F_v/f_m , qP , and *NPQ* were observed. In the combined exposure, the 2 W-ANOVA identified significant interactions between the two stressors in terms

of reduction in qP and *NPQ*. The IA prediction and CI overlapping test suggested synergistic interactions between UVB and γ -radiation at 14.9 mGy h⁻¹ and 43.6 mGy h⁻¹ for *NPQ*, respectively, whereas

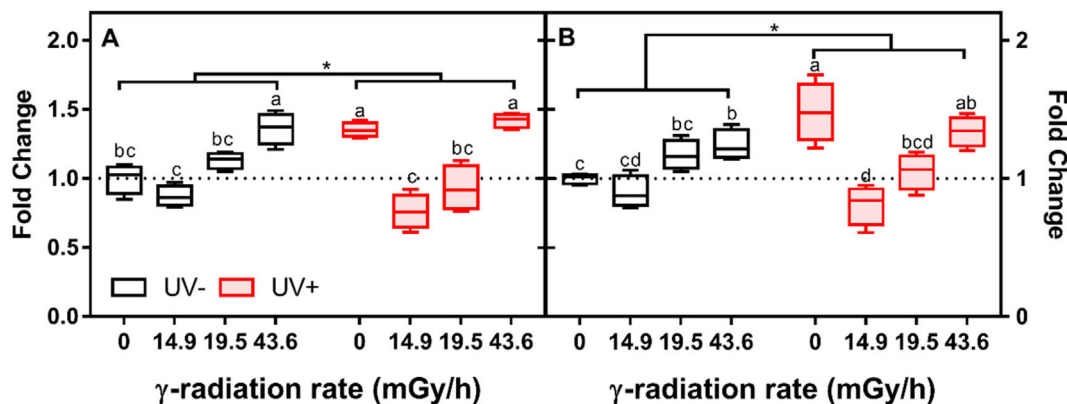


Fig. 3. Effect of gamma radiation on *Lemna minor* growth after exposure with (UV+) or without UVB (UV-) for 7 days: (A) ROS formation and (B) lipid peroxidation (LPO). Boxes represent the median ($N = 6$) and the 25th and 75th percentiles, and the whiskers represent the minimum and maximum value. The dotted line indicates the base level of responses in the control group. Different letters indicate significant differences in means between treatments, while the asterisk “*” denotes significant interaction between groups with or without UVB ($p \leq 0.05$).

synergistic interaction for qP at 19.5 mGy h^{-1} . The 2 W-ANOVA and IA modelling indicated that the UVB caused no enhancement of γ -radiation induced inhibition of F_v/f_m , while causing an additive effect on Φ_{PSII} when exposed in combination (Table 2).

3.5. Pigment content

When exposed to single stressors, γ -radiation caused a dose rate dependent reduction in the chlorophyll content (chlorophyll *a* (Chl *a*) and chlorophyll *b* (Chl *b*), but had no effects on total carotenoids (Fig. 6). A maximum reduction of Chl *a* (0.7-fold) and Chl *b* (0.7-fold) were observed at dose rates of 43.6 mGy h^{-1} . UVB exposure reduced the content of Chl *b* by 20 % when exposed alone, while no significant effect was observed on Chl *a* and the total content of carotenoids. When exposed in combination, no interactions between the two stressors were identified by the 2 W-ANOVA in terms of changes to Chl *a*, Chl *b* or total content of carotenoids. The IA modelling and CI overlapping test verified that the combined effects occurred in a non-enhancement manner for these pigments (Table 2).

3.6. Gene expression

When exposed to γ -radiation alone, expression of the antioxidant biomarker gene glutathione-S-transferase (*GST*), the two DNA damage relevant genes DNA damage-repair/tolerant protein (*DRT111*) and serine threonine-protein kinases (*ATM*), apoptosis relevant genes apoptosis inhibitor 5-like (*API5*), chlorophyll metabolism gene chlorophyllase-2 (*CHL*),

and metacaspase-1 (*AMC1*) were increased at 43.6 mGy h^{-1} (Fig. 7). The D1 protein synthesis gene (*PSBA*), glycolysis enzyme pyruvate kinase (*PK*) and electron transfer enzyme NADH dehydrogenase (*NDUFV1*) were significantly down-regulated in *L. minor* after exposure to γ -radiation at high dose rates ($\geq 20 \text{ mGy h}^{-1}$). The expression of superoxide dismutase (*SOD*), glutathione peroxidase (*GPX*), DNA repair protein rad50 (*RAD50*), D1 protein synthesis gene (*PSBA*), phytoene synthase (*PSY75B*), flavonoid 3'-monooxygenase (*CYP*), cytochrome *c* (*CYC*) and ATP synthase gamma (*ATPC1*) was not significantly affected by γ -radiation when exposed alone. The expression of glycolysis enzyme pyruvate kinase (*PK*) was non-monotonic, with up-regulation at 14.9 mGy h^{-1} and recovery at 20 mGy h^{-1} . Single UVB radiation up-regulated the expression of *AMC1* and *API5*, whereas none of the other genes was differentially expressed compared to the control. When co-exposed to the two stressors, significant interactions were observed between γ -radiation and UVB in terms of modulating the expression of the genes *GST*, *AMC1*, *API5*, *PSBA*, *CHL*, *PK1* and *NDUFV1* (determined by the 2 W-ANOVA). The IA prediction and CI overlapping test revealed synergistic interactions between the two stressors with respect to the increase in *GST* and decreased in *PSBA*, whereas regulation of the genes *ATM*, *AMC1*, *CHL*, *PK1* and *DNUFV1* occurred in an antagonistic manner (Table 2).

4. Discussion

The individual and combined effects of γ -radiation and UVB were investigated in *L. minor* at multiple levels of biological organisation. Putative

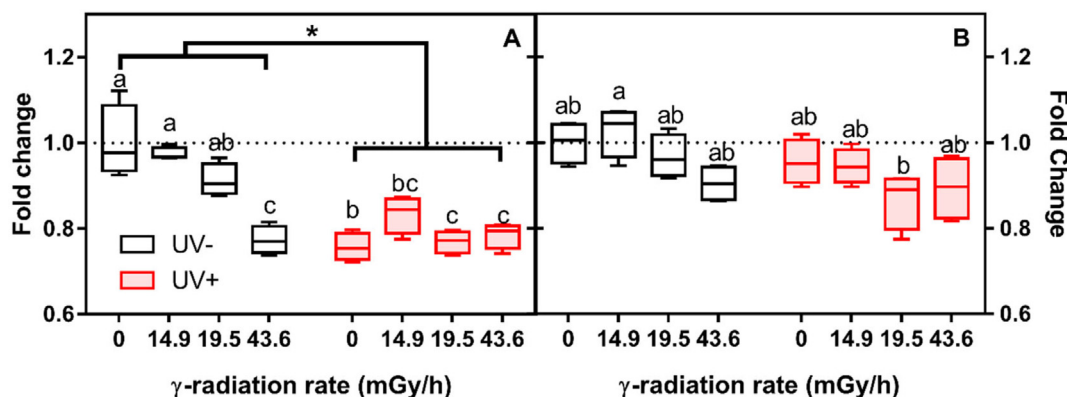


Fig. 4. Effect of gamma radiation on *Lemna minor* growth after exposure with (UV+) or without UVB (UV-) for 7 days: (A) OXPHOS and (B) ATP content. Boxes represent the median ($N = 6$) and the 25th and 75th percentiles, and the whiskers represent the minimum and maximum value. The dotted line indicates the base level of responses in the control group. Different letters indicate significant differences in means between treatments, while the asterisk “*” denotes significant interaction between groups with or without UVB ($p \leq 0.05$).

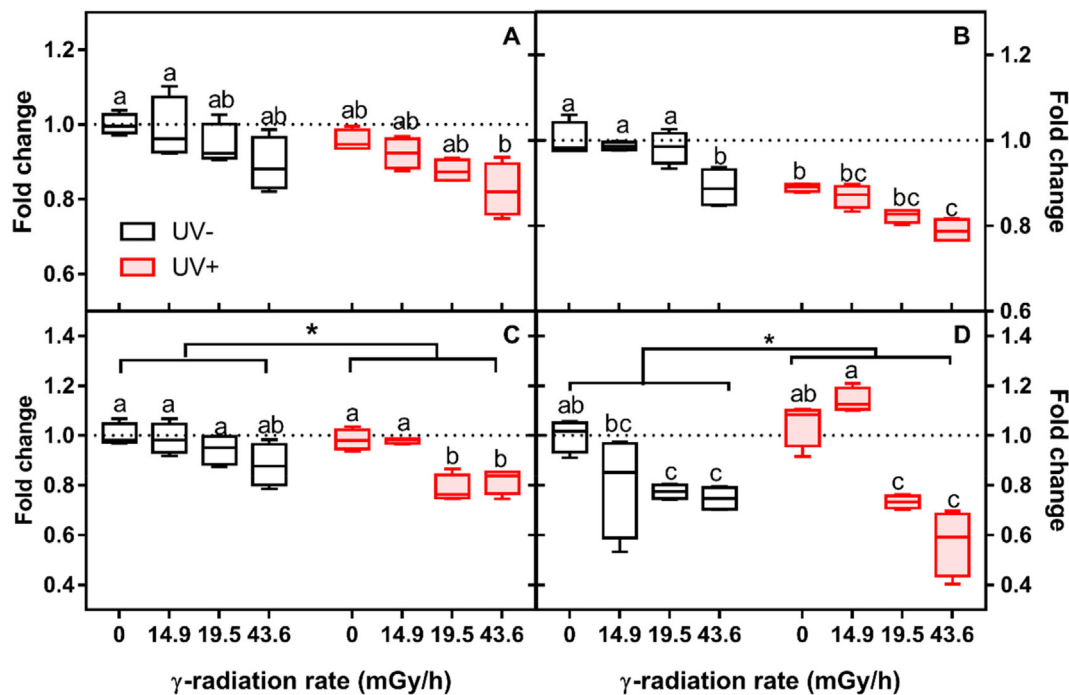


Fig. 5. Effect of gamma radiation on *Lemna minor* growth after exposure with (UV+) or without UVB (UV-) for 7 days: (A) maximal PSII efficiency (F_v/F_m), (B) effective PSII efficiency (Φ_{PSII}), (C) photochemical quenching (qP) and (D) non-photochemical quenching (NPQ). Boxes represent the median ($N = 6$) and the 25th and 75th percentiles, and the whiskers represent the minimum and maximum value. The dotted line indicates the base level of responses in the control group. Different letters indicate significant differences in means between treatments, while the asterisk “*” denotes significant interaction between groups with or without UVB ($p \leq 0.05$).

toxicity pathways have previously been proposed for the single stressors γ -radiation and UVB in *L. minor* (Xie et al., 2019; Xie et al., 2020), and these were used to characterise the combined effects occurring after co-exposures with the two stressors. Compared to the previous study using continuous UVB radiation, the present study was executed with a photoperiod of 16 h daily for UVB radiation, representing a 25 % reduction in total UVB dose (Xie et al., 2020). Although the total daily UVB dose was 2 times higher than that encountered in the central and northern Europe during the peak UVB season (high summer), the UVB irradiance used in the present study was typically in the range of common UV levels observed in Norway ($0.2\text{--}1\text{ W m}^{-2}$) at noon in summer (Johnsen, 2022). The applied dose rates of external γ -radiation in the present study were 0.9 to 4.2 times that observed in the vicinity of the damaged reactor during the first two weeks after the Chernobyl nuclear power plant accident (Fesenko et al., 2005), and were considered a worst-case scenario. Although the γ -radiation and UVB exposure used was in the higher range of what has been encountered in the environment, the main purpose of the studies was to demonstrate mechanistically-informed combined toxicity assessment using γ -radiation

and UVB as prototypical stressors rather than fully represent ecologically relevant exposure scenarios.

4.1. Oxidative stress and damage

Excessive ROS is often accompanied by an increase in the expression of different detoxification compounds (e.g. antioxidant enzymes and phenolic compounds) and damage to biological macromolecules (e.g. lipids) (Babu et al., 2003; Huang et al., 2019; Jansen et al., 2001). In the presented study, significant induction of ROS formation and lipid peroxidation (MDA content) were observed after exposure to γ -radiation at 43.6 mGy h^{-1} , as well as the artificial UVB at 0.49 W m^{-2} , thus suggesting oxidative stress and lipid peroxidation were occurring at high dose rates and irradiance in *L. minor*. The finding is consistent with earlier observation for some of the same markers of effects in *L. minor* after exposure to similar dose rates and irradiance of γ -radiation and UVB (Xie et al., 2019; Xie et al., 2020). Exposure to somewhat lower dose rates from the same source (4.5 mGy h^{-1}) caused ROS in other freshwater primary producers

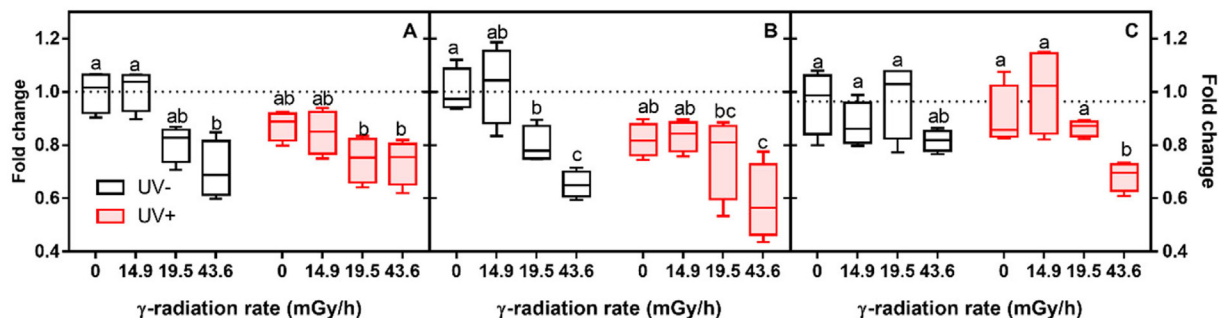


Fig. 6. Effect of gamma radiation on *Lemna minor* growth after exposure with (UV+) or without UVB (UV-) for 7 days: (A) chlorophyll a (Chl a), (B) chlorophyll b (Chl b) and (C) total carotenoids. Boxes represent the median ($N = 6$) and the 25th and 75th percentiles, and the whiskers represent the minimum and maximum value. The dotted line indicates the base level of responses in the control group. Different letters indicate significant differences in means between treatments, while the asterisk “*” denotes significant interaction between groups with or without UVB ($p \leq 0.05$).

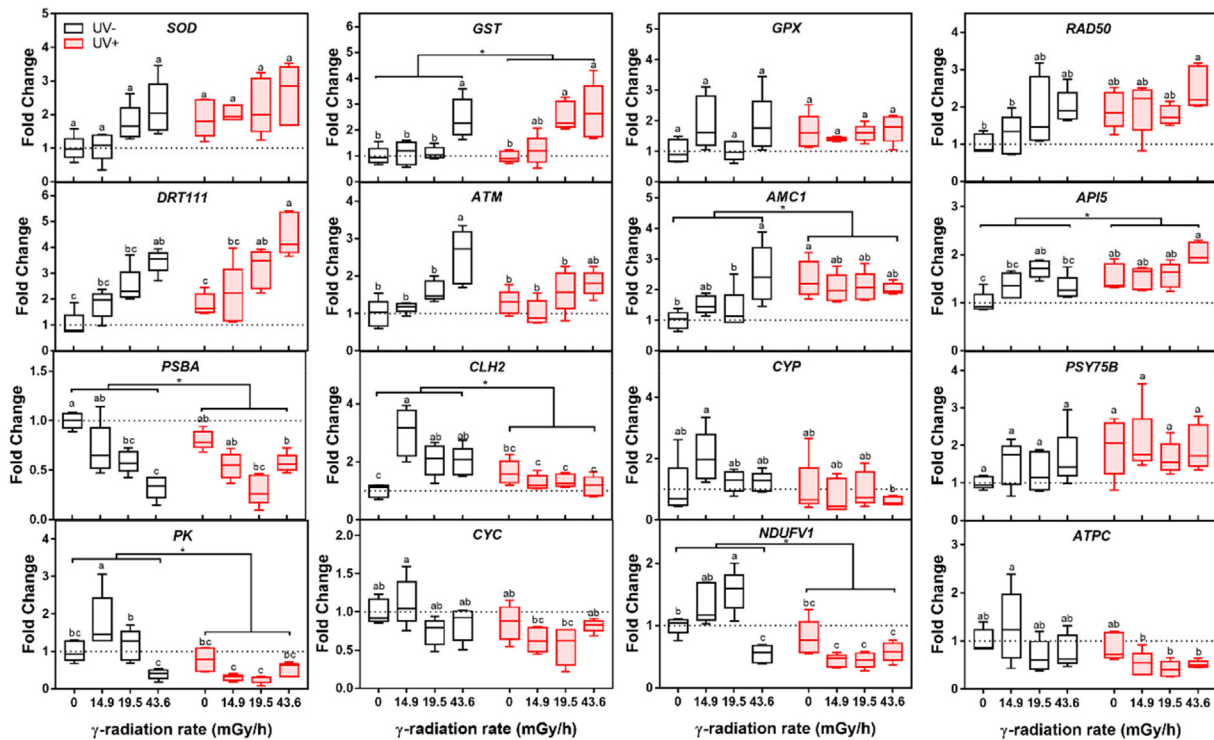


Fig. 7. Effects of gamma radiation on relative transcript levels in *Lemna minor* after exposure with (UV+) or without UVB (UV-) for 7 days. SOD-Superoxide dismutase; GST- Glutathione s-transferase; GPX- Glutathione peroxidase; RAD50- DNA repair protein rad50; ATM-DNA double-strand break sensor; AMC1- Metacaspase-1; API5- apoptosis inhibitor 5; DRT111- DNA-damage repair/tolerance protein 111; PSBA- Photosystem II protein D1; CLH- Chlorophyllase; CYP- Flavonoid production; PSY75B- Carotenoids biosynthesis; PK- Pyruvate kinase; CYC- Cytochrome c; NDUFV1- NADH dehydrogenase; ATPC-ATP synthase gamma. The data is derived from quantitative real-time reverse transcription-polymerase chain reaction (qRT-PCR, white box, N = 6) analyses. The transcript levels were normalised against housekeeping gene glyceraldehyde 3-phosphate dehydrogenase (GADPH), 40s ribosomal protein S18 (RPS18), and elongation factor 1- α (EF1 α) and are shown relative to the non-UV control (shown as a dotted line). Boxes represent the median and the 25th and 75th percentiles, and the whiskers represent the minimum and maximum value. Different letters indicate significant differences in means between treatments, while the asterisk “**” denotes significant interaction between groups with or without UVB ($p \leq 0.05$).

such as the microalgae *Chlamydomonas reinhardtii* (Gomes et al., 2017). The higher sensitivity of microalgae to stressors has previously been attributed to less complex physiological structure and regulatory systems in algae compared to floating macrophytes (Lewis and Thursby, 2018). When co-exposed, the IA assessment suggested that UVB antagonised γ -radiation-mediated effects on ROS formation and MDA content at all dose rates. A similar antagonistic effect on ROS was also observed in the Scots pine (*P. sylvestris*) after combined exposure to γ -radiation and UVB radiation (Blagojevic et al., 2019). Induction of protective mechanisms, such as antioxidant enzymes and phenolic compounds, are normally regulated by ROS signalling, and are known to reduce ROS in aquatic primary producers (Khan et al., 2018). Although no-clear enhancement of *SOD*, *GPX* and *CYP* gene expression was observed, a synergistic up-regulation of the antioxidant enzyme gene *GST* may provide a potential explanation for the antagonistic effect observed (Suppl. Fig. S1). Additionally, the interaction of UVB at the highest γ -radiation dose rate (43.6 mGy h⁻¹) can be also potentially due to saturation of endogenous ROS formation via redox cycling as both γ -radiation and UVB can trigger this in plants (Hideg et al., 2013; Jan et al., 2012).

4.2. DNA damage and programmed cell death

In the plant cells, DNA is one of the major targets for both UVB (Jansen et al., 1998) and γ -radiation (Caplin and Willey, 2018). In this study, the expression of DNA damage marker genes *DRT111* (DNA damage repair) and *ATM* (double-strand break sensor) were all significantly upregulated by γ -radiation at 43.6 mGy h⁻¹, thus suggesting an increase in DNA damage in *L. minor*. γ -induced DNA damage was also observed in *L. minor* after exposure to 24 mGy h⁻¹ γ -radiation (Xie et al., 2019). Exposure to UVB alone did not cause any significant increase in the expression of the same

genes, thus suggesting that induction of DNA strand breaks or induction of DNA damage and repair genes may require exposure to higher UVB irradiances. Unlike γ -radiation, UVB radiation is known to induce photoproducts like CPD (Gill et al., 2015), which was consistent with the observations of an increase in CPD at 0.48 W m⁻² (estimated 1.3 times higher accumulated dose than the present study) in *L. minor* (Xie et al., 2020). No interaction (2 W-ANOVA) and no enhancement of effects (IA modelling) were observed for the expression of *ATM*, *RAD50* and *DRT111* when exposed to the two stressors in combination. No-enhancement on the DNA damage marker genes could be expected as UVB irradiance did not cause any significant increase in DNA damage (Fig. 7). Additionally, the different MoAs of γ and UVB in terms of DNA damage may also explain the non-interactions observed. More specifically, γ -radiation-mediated DNA double-strand breaks are typically caused by the destruction of sugar-phosphate backbones or disruption of the base pairs of the DNA molecule through direct energy dissipation (Singh et al., 2011), while UVB-induced DNA double-strand breaks in plants are normally caused indirectly by either increased oxidative stress, or induction of CPD formation (Suppl. Fig. S2) (Rastogi et al., 2010).

Consequently, increased DNA damage could lead to PCD as a secondary response, thereby protecting organisms from radiation-damaged cells (Pennell and Lamb, 1997). In the present study, increased transcription of *API5* (apoptosis inhibitor) and *AMC1* (metacaspases) were observed after exposure to γ -radiation (19.5–43.6 mGy h⁻¹) and UVB (0.49 W m⁻²), potentially indicating induction of PCD in *L. minor*. Although not investigated in *L. minor* before, γ -mediated PCD following DNA damage has been well documented in *Arabidopsis thaliana* (Furukawa et al., 2010 #144). In accordance with the present results, up-regulation of transcripts for *API5* and *AMC1* were observed in *L. minor* after exposure to 0.48 and 1 W m⁻² UVB, respectively (Xie et al., 2020). Interestingly, IA assessment suggested

that UVB modulated γ -radiation-mediated expression of PCD marker genes, where additive effects were identified at 19.5 mGy h^{-1} while antagonistic effects were demonstrated at 14.9 and 43.6 mGy h^{-1} . The combined effects trends on PCD are not consistent with the expression of DNA damage marker genes, and the observed non-monotonic behaviour in PCD at different dose rates in the combined exposures may suggest activation of different toxicity mechanisms (Suppl. Fig. S3). In addition to DNA damage, PCD in plants is additionally regulated by ROS signalling, mitochondrial dysfunction, and phytohormones in plants (Balk et al., 1999; Redza-Dutordoir and Averill-Bates, 2016; Steffens and Sauter, 2005). However, the details of the toxicity mechanism associated with PCD in the present study remain unresolved and warrant additional experimental assessments.

4.3. Performance of photosystem II

Photosystem II (PSII) is a protein complex in the light-dependent reaction, which can split water to form protons, oxygen, and electron for photosynthesis (Aro et al., 1993). After exposure, a significant reduction of effective PSII efficiency (Φ_{PSII} , 43.6 mGy h^{-1}), non-photochemical quenching (NPQ, $19.5\text{--}43.6 \text{ mGy h}^{-1}$), D1 protein (PSBA, $19.5\text{--}43.6 \text{ mGy h}^{-1}$), the content of chlorophyll *a* (Chl *a*, 43.6 mGy h^{-1}) and *b* (Chl *b*, $19.5\text{--}43.6 \text{ mGy h}^{-1}$) were all observed in *L. minor* after exposure to γ -radiation. The results are consistent with earlier observations for many of the same markers of effects in *L. minor* exposed to similar dose rates and suggest that elevated γ -radiation may potentially reduce the photosynthesis in aquatic plants (Xie et al., 2019). UVB at 0.49 W m^{-2} only cause significant inhibition of effective PSII efficiency (Φ_{PSII}), which agrees with observation in *L. minor* after exposure to similar UVB irradiance (Xie et al., 2020). Interestingly, the 2 W-ANOVA and IA assessment demonstrated that UVB induced additive inhibition of Φ_{PSII} when co-exposed with γ -radiation at all dose rates, while synergistic interactions were observed in NPQ and qP at different dose rates. The variable combined effects at different markers can be potentially due to the two stressors modulating PSII performance via distinct toxicity mechanisms (Suppl. Fig. S4). Mechanistic studies have indicated that artificial γ -radiation and UVB radiation can cause damage to photoreaction reaction centres (Caplin and Willey, 2018) and the oxygen evolution complex (OEC) at donor sites, respectively (Hideg and Vass, 1996; Ohnishi et al., 2005). Decreased D1 protein synthesis can be another potential reason for the PSII inhibition, as the modulation of D1 protein recovery impacts the overall function of PSII (Aro et al., 1993). Additionally, the activity of PSII is regulated by the rate of photon absorption in the light-harvesting complex (LHC) (Pätsikkä et al., 2002), and the reduction of total chlorophylls may thus render the leaves more susceptible to photoinhibition due to their role as photoreceptors in the chloroplast.

4.4. Oxidative phosphorylation and content of ATP

Oxidative phosphorylation (OXPHOS) is a metabolic pathway mainly for ATP production in eukaryotic cells (Terada, 1990). In the present study, significant inhibition of MMP was observed after exposure to single γ -radiation (43.6 mGy h^{-1}) and UVB at 0.49 W m^{-2} . Suppression of MMP has been observed previously in the same species after exposure to 24 mGy h^{-1} γ -radiation (Xie et al., 2019) and UVB at 1 W m^{-2} (Xie et al., 2020), thus suggesting that the two stressors reduce OXPHOS in *L. minor*. The slightly different results between studies may potentially be due to the exposure setup with varying durations of exposure and light sources. When co-exposed, 2 W-ANOVA and IA model demonstrated that UVB antagonistically modulate the effects of γ -radiation on MMP at all dose rates. Such antagonistic reduction can be potentially due to the ROS-mediated damage to the inner mitochondrial membrane (Jugé et al., 2016; Fraikin, 2018a) (Suppl. Fig. S5). Alternatively, both γ -radiation and UVB were reported to inhibit the electron flow between OXPHOS complexes, which may lead to competition in the electron transport (Kam and Banati, 2013; Gniadecki et al., 2000). The reduction of OXPHOS is consequently expected to reduce the production of ATP (Reape et al., 2008). Surprisingly, exposure to

γ -radiation or UVB alone did not affect the total ATP content and the expression of ATP synthase (*ATPCT1*). The 2 W-ANOVA and IA model also indicated that UVB caused no-enhancement of ATP content and expression of ATP synthase (*ATPCT1*) when co-exposed with γ -radiation. Such combined effects cannot be fully explained by PSII (additive reduction), MMP (antagonistic reduction) and glycolysis (antagonistic reduction on the expression of Pyruvate kinase (*PK*)) (Suppl. Fig. S6). Additional studies to decipher the combined effect of the two stressors on ATP, photophosphorylation, OXPHOS and glycolysis are clearly warranted.

4.5. Apical effects on growth and reproduction

As an adverse outcome, responses of growth parameters in *L. minor*, including reproduction and developments, have been widely used as standardised toxicity endpoints with different environmental stressors (Germ and Gaberscik, 1999; Radić et al., 2011). The present study showed that γ -radiation significantly inhibited the frond number (FN, 43.6 mGy h^{-1}), frond size (FS, $19.5\text{--}43.6 \text{ mGy h}^{-1}$) and frond weight (FW, $19.5\text{--}43.6 \text{ mGy h}^{-1}$) (Suppl. Table. S3). This is consistent with the observations that γ -radiation reduced reproduction in *L. minor* after exposure to 50 mGy h^{-1} (Ivanishvili et al., 2016), and suppressed frond size and weight at 24 mGy h^{-1} (Xie et al., 2019). As observed earlier (Xie et al., 2019; Van Hoeck et al., 2015), individual growth endpoints (FS and FW) were more sensitive to γ -radiation than reproduction (FN). Exposure to UVB alone did not cause any significant effects on the three apical endpoints in *L. minor*, suggesting that higher UVB irradiances would be required to cause adverse effects. Interestingly, the 2 W-ANOVA and IA model demonstrated that UVB caused a synergistic reduction in reproduction (FN) when co-exposed with γ -radiation at all dose rates, while no-enhancement was observed in individual growth (FW and FS). Although the combined effect of γ -radiation and UVB on aquatic plants has not been investigated extensively, the combination of γ -radiation and cadmium was also shown to synergistically reduce the cell biomass of microalgae *R. subcapitata* (Bradshaw et al., 2019), which suggested that more than additive effects between γ -radiation and other stressors may be prevalent at the apical level (i.e. adverse effects). Plant development and growth are regulated by various physiological responses at the cellular and subcellular levels, such as energy metabolism, PCD, and phytohormones (Grover et al., 2001), which suggest that propagation of interactions from multiple levels of biological organisation (Suppl. Fig. S7) are highly likely, albeit seldom characterised.

4.6. Putative toxicity pathways

The major toxicity pathways modified by γ -radiation and UVB have previously been proposed for *L. minor* using similar experimental setups and effect methods (Xie et al., 2019; Xie et al., 2020). These studies have proposed that the stressors can cause growth inhibition through different MoAs, including induction of oxidative stress and DNA damage, and inhibition of photosynthesis and OXPHOS when exposed alone (Suppl. Fig. S8). In the present study, a set of putative toxicity pathways were proposed to evaluate the combined effects of the two stressors across multiple levels of biological organisation (Fig. 8 and Suppl. Fig. S9). As an initial response, UVB did not alter γ -mediated DNA damage but antagonised γ -radiation in terms of ROS formation and thus likely also LPO formation. The combined effects on the inhibition of PSII could be associated with the reduction of chlorophylls and potentially also D1 protein turnover (although not assessed herein). Interestingly, most combined effects occurring at the subcellular and cellular levels displayed non-interaction (either additive or no-enhancement) or antagonistic effects of the stressors, albeit the combined effect at the apical level showed either synergistic interaction (i.e. for reproduction (FN)) or no-enhancement (i.e. growth parameters such as FS and FA). Although the underlying responses at the subcellular or cellular level were not studied in sufficient detail to provide a complete linkage between the responses, it can be hypothesised that a combination of cell regeneration following PCD and DNA damage, deactivation of photophosphorylation and OXPHOS in mitochondrial and chloroplast affected energy generation and

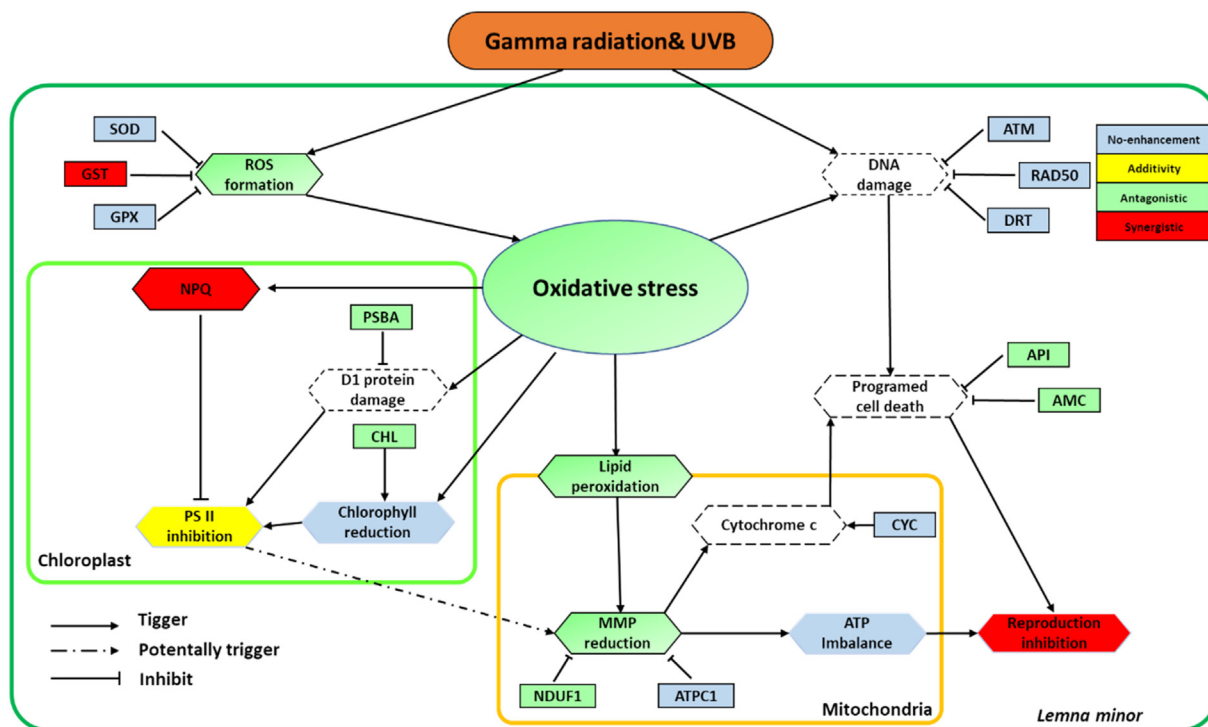


Fig. 8. Generalised putative toxicity mechanism in aquatic plant *Lemna minor* after exposure to a combination of γ -radiation and UVB for 7 days. No-enhancement, additive, antagonistic, and synergistic interactions were colour-coded as blue, yellow, green and red, respectively. Dose rate- and target-specific responses are provided in detail in suppl. Fig. S9.

restricted available energy for development and reproduction (Calow, 1991; De Col et al., 2017). As both UVB and γ -radiation induce effects through a number of pathways, it is challenging to elucidate the exact mechanism(s) for the UVB enhancement of γ -mediated effects at the apical level (i.e. reproduction) on the basis of results from the present study alone. The antagonistic interactions on PCD were considered a key process leading to growth inhibition of *L. minor*, as this process is involved in the regulation of development and cell survival (Sparks et al., 2013; De Col et al., 2017). The change of the ATP pool could be an additional factor that influenced growth as energy metabolism is also involved in cell division and development (Calow, 1991). Generally, ATP in plant cells is generated by different metabolic pathways, including photophosphorylation, glycolysis, and OXPHOS. The synergistic inhibition of reproduction may thus potentially be a compensatory mechanism involving an increase in ATP demand due to oxidative stress, LPO and DNA damage. Although not investigated in the present study, γ -radiation and/or UVB could potentially inhibit reproduction and frond development by affecting the accumulation of phytohormones, including abscisic acid (ABA), gibberellins (GAs), indoleacetic acid (IAA) in plants (Newton, 1977; Qi et al., 2015; Rakitin et al., 2008).

5. Conclusion

The present study provided demonstration of how a combination of experimental and computational methods can enhance our mechanistic understanding of how UVB modulates the stress responses induced by γ -radiation at multiple levels of biological organisation in *L. minor*. The results demonstrated that the combined effects (no-enhancement, additivity, antagonism and synergism) of UVB radiation and γ -radiation were highly dose rate-dependent and target-specific, and supported the hypothesis that interaction such as synergism was more consistently observed across dose rates at the higher organisational level (e.g. reduction in reproduction), whereas more dose rate-dependent combined effects were observed at the cellular or sub-cellular levels. Although the exact mechanisms were not described in detail, the present study showed how a combination of experimental studies and assessment of combined toxicity using statistical and mathematical models

could quantify the interactions occurring and pinpoint endpoints susceptible to combined effects in *L. minor*. The putative toxic pathways proposed suggest propagation of combined effects of the stressors from subcellular responses to adverse effects and represent an initial effort to enhance the understanding of how ionizing and non-ionizing radiation pose cumulative hazards to aquatic plants. Subsequent efforts to assess the combined effects of multiple stressors, such as ionizing and non-ionizing radiation, are anticipated to focus on typical environmental exposure scenarios using experimental and computational efforts demonstrated herein.

CRedit authorship contribution statement

K. E. Tollefsen and L. Xie contributed to the conception of the study; L. Xie and Y. Song, K. A. Solhaug, O. C. Line, and D. A. Brede performed the experiments; L. Xie, Y. Song and K. Petersen processed the experimental data and performed the analysis; B. Salbu supervised the project; L. Xie and K. E. Tollefsen wrote the manuscript with the input from all authors; All authors read and approved the final manuscript.

Declaration of competing interest

The authors declare that they have no known competing financial interests or personal relationships that could have appeared to influence the work reported in this paper.

Acknowledgements

Funding from the Research Council of Norway through its Centres of Excellence funding scheme, project number 223268, and NIVA's Computational Toxicology Program, NCTP (www.niva.no/nctp, RCN project number 160016) is gratefully acknowledged. The authors acknowledge the assistance from professor Jorunn Elisabeth Olsen (Norwegian University of Life Sciences, NMBU) for the internal review of this manuscript. Lastly, we would like to pay our gratitude and our respects to our engineer Dag Wenner (†), who designed and built the climate chambers.

Appendix A. Supplementary data

Supplementary data to this article can be found online at <https://doi.org/10.1016/j.scitotenv.2022.157457>.

References

- Alikamanoglu, S., Yacili, O., Sen, A., 2011. Effect of gamma radiation on growth factors, biochemical parameters, and accumulation of trace elements in soybean plants (*Glycine max* L. Merrill). *Biol. Trace Elem. Res.* 141 (1–3), 283–293. <https://doi.org/10.1007/s12011-010-8709-y>.
- Aro, E.M., McCaffery, S., Anderson, J.M., 1993. Photoinhibition and D1 protein degradation in peas acclimated to different growth irradiances. *Plant Physiol.* 103 (3), 835–843. <https://doi.org/10.1104/pp.103.3.835>.
- Babu, T.S., Akhtar, T.A., Lampi, M.A., Tripuranthakam, S., Dixon, D.G., Greenberg, B.M., 2003. Similar stress responses are elicited by copper and ultraviolet radiation in the aquatic plant *Lemma gibba*: implication of reactive oxygen species as common signals. *Plant Cell Physiol.* 44 (12), 1320–1329. <https://doi.org/10.1093/pcp/pcg160>.
- Baker, N.R., 2008. Chlorophyll fluorescence: a probe of photosynthesis in vivo. *Annu. Rev. Plant Biol.* 59, 89–113. <https://doi.org/10.1146/annurev.arplant.59.032607.092759>.
- Balk, J., Leaver, C.J., McCabe, P.F., 1999. Translocation of cytochrome c from the mitochondria to the cytosol occurs during heat-induced programmed cell death in cucumber plants. *FEBS Lett.* 463 (1–2), 151–154. [https://doi.org/10.1016/s0014-5793\(99\)01611-7](https://doi.org/10.1016/s0014-5793(99)01611-7).
- Bernhard, G.H., Neale, R.E., Barnes, P.W., Neale, P.J., Zepp, R.G., Wilson, S.R., Andrady, A.L., Bais, A.F., McKenzie, R.L., Aucamp, P.J., Young, P.J., Liley, J.B., Lucas, R.M., Yazar, S., Rhodes, L.E., Byrne, S.N., Hollestein, L.M., Olsen, C.M., Young, A.R., Robson, T.M., Bornman, J.F., Jansen, M.A.K., Robinson, S.A., Ballare, C.L., Williamson, C.E., Rose, K.C., Banaszak, A.T., Hader, D., Hylander, S., Wangberg, S., Austin, A.T., Hou, W., Paul, N.D., Madronich, S., Sulzberger, B., Solomon, K.R., Li, H., Schikowski, T., Longstreth, J., Pandey, K.K., Heikkila, A.M., White, C.C., 2020. Environmental effects of stratospheric ozone depletion, UV radiation and interactions with climate change: UNEP environmental effects assessment panel, update 2019. *Photochem. Photobiol. Sci.* 19 (5), 542–584. <https://doi.org/10.1039/d0pp90011g>.
- Bjerke, H., Hetland, P.O., 2014. Dosimetri ved FIGARO gammaanlegget ved NMBU, ÅS. Målerapport fra oppmåling av doseraten i strålefeltet fra kobolt-60 NRPA Technical Document Series 2.
- Blagojevic, D., Lee, Y., Xie, L., Brede, D.A., Nybakken, L., Lind, O.C., Tollefsen, K.E., Salbu, B., Solhaug, K.A., Olsen, J.E., 2019. No evidence of a protective or cumulative negative effect of UV-B on growth inhibition induced by gamma radiation in Scots pine (*Pinus sylvestris*) seedlings. *Photochem. Photobiol. Sci.* 18 (8), 1945–1962. <https://doi.org/10.1039/c8pp00491a>.
- Bliss, C.I., 1939. The toxicity of poisons applied JOINTLY. *Ann. Appl. Biol.* 26 (3), 585–615. <https://doi.org/10.1111/j.1744-7348.1939.tb06990.x>.
- Bornman, J.F., Barnes, P.W., Robson, T.M., Robinson, S.A., Jansen, M.A., Ballare, C.L., Flint, S.D., 2019. Linkages between stratospheric ozone, UV radiation and climate change and their implications for terrestrial ecosystems. *Photochem. Photobiol. Sci.* 18 (3), 681–716.
- Bradshaw, C., Meseh, D.A., Alasawi, H., Qiang, M., Snoeijis-Leijonmalm, P., Nascimento, F.J.A., 2019. Joint effects of gamma radiation and cadmium on subcellular-, individual- and population-level endpoints of the green microalgae *Raphidocelis subcapitata*. *Aquat. Toxicol.* 211, 217–226. <https://doi.org/10.1016/j.aquatox.2019.04.008>.
- Calow, P., 1991. Physiological costs of combating chemical toxicants: ecological implications. *Comp. Biochem. Physiol. C Comp. Pharmacol. Toxicol.* 100 (1–2), 3–6. [https://doi.org/10.1016/0742-8413\(91\)90110-f](https://doi.org/10.1016/0742-8413(91)90110-f).
- Caplin, N., Willey, N., 2018. Ionizing radiation, higher plants, and radioprotection: from acute high doses to chronic low doses. *Front. Plant Sci.* 9, 847. <https://doi.org/10.3389/fpls.2018.00847>.
- Cochran, T.B., Norris, R.S., Suokko, K.L., 1993. Radioactive Contamination at Chelyabinsk-65, Russia. Annual Reviews Inc, United States.
- Czegeny, G., Matai, A., Hideg, E., 2016. UV-B effects on leaves-oxidative stress and acclimation in controlled environments. *Plant Sci.* 248, 57–63. <https://doi.org/10.1016/j.plantsci.2016.04.013>.
- De Col, V., Fuchs, P., Nietzel, T., Elsässer, M., Voon, C.P., Candeo, A., Seeliger, I., Fricker, M.D., Grefen, C., Möller, I.M., Bassi, A., Lim, B.L., Zancani, M., Meyer, A.J., Costa, A., Wagner, S., Schwarzländer, M., 2017. ATP sensing in living plant cells reveals tissue gradients and stress dynamics of energy physiology. *eLife* 6, e26770. <https://doi.org/10.7554/eLife.26770>.
- Fesenko, S.V., Alexakhin, R.M., Geras'kin, S.A., Sanzharova, N.I., Spirin, Y.V., Spiridonov, S.I., Gontarenko, I.A., Strand, P., 2005. Comparative radiation impact on biota and man in the area affected by the accident at the Chernobyl nuclear power plant. *J. Environ. Radioact.* 80 (1), 1–25. <https://doi.org/10.1016/j.jenvrad.2004.08.011>.
- Fraikin, G.Y., 2018a. Signaling mechanisms regulating diverse plant cell responses to UVB radiation. *Biochem. Mosc.* 83 (7), 787–794. <https://doi.org/10.1134/S0006297918070027>.
- Fraikin, G.Y., 2018b. Signaling mechanisms regulating diverse plant cell responses to UVB radiation. *Biochem. Mosc.* 83 (7), 787–794. <https://doi.org/10.1134/S0006297918070027>.
- Furukawa, T., Curtis, M.J., Tominey, C.M., Duong, Y.H., Wilcox, B.W.L., Aggoune, D., Hays, J.B., Britt, A.B., 2010. A shared DNA-damage-response pathway for induction of stem-cell death by UVB and by gamma irradiation. *DNA Repair* 9 (9), 940–948. <https://doi.org/10.1016/j.dnarep.2010.06.006>.
- Germ, M., Gaberscik, A., 1999. The effect of UV-B radiation and nutrient availability on growth and photochemical efficiency of PS II in common duckweed. *Phyton-Horn* 39 (3), 187–192.
- Gill, S.S., Anjum, N.A., Gill, R., Jha, M., Tuteja, N., 2015. DNA damage and repair in plants under ultraviolet and ionizing radiations. *TheScientificWorldJOURNAL* 2015, 250158. <https://doi.org/10.1155/2015/250158>.
- Gniadecki, R., Thorn, T., Vicanova, J., Petersen, A., Wulf, H.C., 2000. Role of mitochondria in ultraviolet-induced oxidative stress. *J. Cell. Biochem.* 80 (2), 216–222. [https://doi.org/10.1002/1097-4644\(20010201\)80:2<216::aid-jcb100>3.0.co;2-h](https://doi.org/10.1002/1097-4644(20010201)80:2<216::aid-jcb100>3.0.co;2-h).
- Gomes, T., Xie, L., Brede, D., Lind, O.C., Solhaug, K.A., Salbu, B., Tollefsen, K.E., 2017. Sensitivity of the green alga *Chlamydomonas reinhardtii* to gamma radiation: photosynthetic performance and ROS formation. *Aquat. Toxicol.* 183, 1–10. <https://doi.org/10.1016/j.aquatox.2016.12.001>.
- Grover, A., Kapoor, A., Lakshmi, O.S., Agarwal, S., Sahi, C., Katiyar-Agarwal, S., Agarwal, M., Dubey, H., 2001. Understanding molecular alphabets of the plant abiotic stress responses. *Curr. Sci.* 80, 206–216.
- Hansen, E.L., Lind, O.C., Oughton, D.H., Salbu, B., 2019. A framework for exposure characterization and gamma dosimetry at the NMBU FIGARO irradiation facility. *Int. J. Radiat. Biol.* 95 (1), 82–89. <https://doi.org/10.1080/09553002.2018.1539878>.
- Hashem, H., 2013. Cadmium toxicity induces lipid peroxidation and alters cytokinin content and antioxidant enzyme activities in soybean. *Botany* 92 (1), 1–7.
- Hideg, É., Vass, I., 1996. UV-B induced free radical production in plant leaves and isolated thylakoid membranes. *Plant Sci.* 115 (2), 251–260. [https://doi.org/10.1016/0168-9452\(96\)04364-6](https://doi.org/10.1016/0168-9452(96)04364-6).
- Hideg, E., Jansen, M.A., Strid, A., 2013. UV-B exposure, ROS, and stress: inseparable companions or loosely linked associates? *Trends Plant Sci.* 18 (2), 107–115. <https://doi.org/10.1016/j.tplants.2012.09.003>.
- Hidema, J., Taguchi, T., Ono, T., Teranishi, M., Yamamoto, K., Kumagai, T., 2007. Increase in CPD photolase activity functions effectively to prevent growth inhibition caused by UVB radiation. *Plant J.* 50 (1), 70–79. <https://doi.org/10.1111/j.1365-313X.2007.03041.x>.
- Hollosoy, F., 2002. Effects of ultraviolet radiation on plant cells. *Micron* 33 (2), 179–197. [https://doi.org/10.1016/s0968-4328\(01\)00011-7](https://doi.org/10.1016/s0968-4328(01)00011-7).
- Huang, H., Ullah, F., Zhou, D.X., Yi, M., Zhao, Y., 2019. Mechanisms of ROS regulation of plant development and stress responses. *Front. Plant Sci.* 10, 800. <https://doi.org/10.3389/fpls.2019.00800>.
- Ivanishvili, N.I., Gogebashvili, M.E., Gvritshvili, N.Z., 2016. Gamma-radiation effect on the parameters of the population recovery of plants. *Ann. Agrar. Sci.* 14 (4), 319–322. <https://doi.org/10.1016/j.aasci.2016.10.005>.
- Jablonski, N.G., Chaplin, G., 2010. Colloquium paper: human skin pigmentation as an adaptation to UV radiation. *Proc. Natl. Acad. Sci. U. S. A.* 107 Suppl 2 (supplement_2), 8962–8968. <https://doi.org/10.1073/pnas.0914628107>.
- Jan, S., Parween, T., Siddiqi, T.O., Mahmoodzafar, 2012. Effect of gamma radiation on morphological, biochemical, and physiological aspects of plants and plant products. *Environ. Rev.* 20 (1), 17–39. <https://doi.org/10.1139/a11-021>.
- Jansen, M.A.K., Gaba, V., Greenberg, B.M., 1998. Higher plants and UV-B radiation: balancing damage, repair and acclimation. *Trends Plant Sci.* 3 (4), 131–135. [https://doi.org/10.1016/S1360-1385\(98\)01215-1](https://doi.org/10.1016/S1360-1385(98)01215-1).
- Jansen, M.A., van den Noort, R.E., Tan, M.Y., Prinsen, E., Lagrimini, L.M., Thorneley, R.N., 2001. Phenol-oxidizing peroxidases contribute to the protection of plants from ultraviolet radiation stress. *Plant Physiol.* 126 (3), 1012–1023. <https://doi.org/10.1104/pp.126.3.1012>.
- Johnsen, B., 2022. GitHub repository. <https://github.com/uvnrpa>.
- Jonker, M.J., Svendsen, C., Bedaux, J.J., Bongers, M., Kammenga, J.E., 2005. Significance testing of synergistic/antagonistic, dose level-dependent, or dose ratio-dependent effects in mixture dose-response analysis. *Environ. Toxicol. Chem.* 24 (10), 2701–2713. <https://doi.org/10.1897/04-431r.1>.
- Jugé, R., Breugnot, J., Da Silva, C., Bordes, S., Closs, B., Aouacheria, A., 2016. Quantification and characterization of UVB-induced mitochondrial fragmentation in normal primary human keratinocytes. *Sci. Rep.* 6 (1), 35065. <https://doi.org/10.1038/srep35065>.
- Kam, W.W., Banati, R.B., 2013. Effects of ionizing radiation on mitochondria. *Free Radic. Biol. Med.* 65, 607–619. <https://doi.org/10.1016/j.freeradbiomed.2013.07.024>.
- Khan, M.I., Shin, J.H., Kim, J.D., 2018. The promising future of microalgae: current status, challenges, and optimization of a sustainable and renewable industry for biofuels, feed, and other products. *Microb. Cell Factories* 17 (1), 36. <https://doi.org/10.1186/s12934-018-0879-x>.
- Kryshev, I.I., Romanov, G.N., Isaeva, L.N., Kholina, Y.B., 1997. Radioecological state of lakes in the southern Ural impacted by radioactivity release of the 1957 radiation accident. *J. Environ. Radioact.* 34 (3), 223–235. [https://doi.org/10.1016/0265-931X\(96\)00033-1](https://doi.org/10.1016/0265-931X(96)00033-1).
- Lewis, M., Thursty, G., 2018. Aquatic plants: test species sensitivity and minimum data requirement evaluations for chemical risk assessments and aquatic life criteria development for the USA. *Environ. Pollut.* 238, 270–280. <https://doi.org/10.1016/j.envpol.2018.03.003>.
- Lichtenthaler, H.K., 1987. [34] chlorophylls and carotenoids: pigments of photosynthetic biomembranes. *Methods in Enzymology* 148. Academic Press, pp. 350–382. [https://doi.org/10.1016/0076-6879\(87\)48036-1](https://doi.org/10.1016/0076-6879(87)48036-1).
- Lind, O.C., Helen Oughton, D., Salbu, B., 2019. The NMBU FIGARO low dose irradiation facility. *Int. J. Radiat. Biol.* 95 (1), 76–81. <https://doi.org/10.1080/09553002.2018.1516906>.
- Lubin, D., Jensen, E.H., Gies, H.P., 1998. Global surface ultraviolet radiation climatology from TOMS and ERBE data. *J. Geophys. Res. Atmos.* 103 (D20), 26061–26091. <https://doi.org/10.1029/98jd02308>.
- Nayek, S., Choudhury, I., Haque, Nishika J., Roy, S., 2014. Spectrophotometric analysis of chlorophylls and carotenoids from commonly grown Fern species by using various extracting solvents. *Res. J. Chem. Sci.* 4, 2231–2606. <https://doi.org/10.1055/s-0003-1340072>.
- Newton, R.J., 1977. Abscisic acid effects on fronds and roots of *Lemma minor* L. *Am. J. Bot.* 64 (1), 45–49. <https://doi.org/10.2307/2441874>.
- OECD, 2006. Test No. 221: *Lemma* sp. Growth Inhibition Test. <https://doi.org/10.1787/9789264016194-en>.

- Ohnishi, N., Allakhverdiev, S.I., Takahashi, S., Higashi, S., Watanabe, M., Nishiyama, Y., Murata, N., 2005. Two-step mechanism of photodamage to photosystem II: step 1 occurs at the oxygen-evolving complex and step 2 occurs at the photochemical reaction center. *Biochemistry* 44 (23), 8494–8499. <https://doi.org/10.1021/bi047518q>.
- Pätsikkä, E., Kairavuo, M., Sersen, F., Aro, E.M., Tyystjärvi, E., 2002. Excess copper predisposes photosystem II to photoinhibition in vivo by outcompeting iron and causing decrease in leaf chlorophyll. *Plant Physiol.* 129 (3), 1359–1367. <https://doi.org/10.1104/pp.004788>.
- Pennell, R.I., Lamb, C., 1997. Programmed cell death in plants. *Plant Cell* 9 (7), 1157–1168. <https://doi.org/10.1105/tpc.9.7.1157>.
- Pfaffl, M.W., 2001. A new mathematical model for relative quantification in real-time RT-PCR. *Nucleic Acids Res.* 29 (9), e45. <https://doi.org/10.1093/nar/29.9.e45>.
- Qi, W., Zhang, L., Feng, W., Xu, H., Wang, L., Jiao, Z., 2015. ROS and ABA signaling are involved in the growth stimulation induced by low-dose gamma irradiation in Arabidopsis seedling. *Appl. Biochem. Biotechnol.* 175 (3), 1490–1506. <https://doi.org/10.1007/s12010-014-1372-6>.
- Radić, S., Stipaničev, D., Cvjetko, P., Mikelić, L.L., Rajčić, M.M., Širac, S., Pevalak-Kozlina, B., Pavlica, M., 2010. *Ecotoxicological assessment of industrial effluent using duckweed (Lemna minor L.) as a test organism.* *Ecotoxicology* 19 (1), 216.
- Radić, S., Stipaničev, D., Cvjetko, P., Marijanović Rajčić, M., Širac, S., Pevalak-Kozlina, B., Pavlica, M., 2011. Duckweed Lemna minor as a tool for testing toxicity and genotoxicity of surface waters. *Ecotoxicol. Environ. Saf.* 74 (2), 182–187. <https://doi.org/10.1016/j.ecoenv.2010.06.011>.
- Rakitin, V.Y., Karyagin, V.V., Rakitina, T.Y., Prudnikova, O.N., Vlasov, P.V., 2008. UV-B stress-induced ABA production in Arabidopsis thaliana mutants defective in ethylene signal transduction pathway. *Russ. J. Plant Physiol.* 55 (6), 854–856. <https://doi.org/10.1134/S1021443708060174>.
- Rastogi, R.P., Richa, Kumar A., Tyagi, M.B., Sinha, R.P., 2010. Molecular mechanisms of ultraviolet radiation-induced DNA damage and repair. *J. Nucleic Acids* 2010, 592980. <https://doi.org/10.4061/2010/592980>.
- Reape, T.J., Molony, E.M., McCabe, P.F., 2008. Programmed cell death in plants: distinguishing between different modes. *J. Exp. Bot.* 59 (3), 435–444. <https://doi.org/10.1093/jxb/erm258>.
- Redza-Dutordoir, M., Averill-Bates, D.A., 2016. Activation of apoptosis signalling pathways by reactive oxygen species. *Biochim. Biophys. Acta* 1863 (12), 2977–2992. <https://doi.org/10.1016/j.bbamcr.2016.09.012>.
- Rozema, J., van de Staaij, J., Björn, L.O., Caldwell, M., 1997. UV-B as an environmental factor in plant life: stress and regulation. *Trends Ecol. Evol.* 12 (1), 22–28. [https://doi.org/10.1016/s0169-5347\(96\)10062-8](https://doi.org/10.1016/s0169-5347(96)10062-8).
- Salbu, B., Teien, H.C., Lind, O.C., Tollefsen, K.E., 2019. Why is the multiple stressor concept of relevance to radioecology? *Int. J. Radiat. Biol.* 95 (7), 1015–1024. <https://doi.org/10.1080/09553002.2019.1605463>.
- Shi, C., Yang, F., Zhu, X., Du, E., Yang, Y., Wang, S., Wu, Q., Zhang, Y., 2016. Evaluation of housekeeping genes for quantitative real-time PCR analysis of *Bradysia odoriphaga* (Diptera: Sciaridae). *Int. J. Mol. Sci.* 17 (7). <https://doi.org/10.3390/ijms17071034>.
- Shuryak, I., 2018. Modeling species richness and abundance of phytoplankton and zooplankton in radioactively contaminated water bodies. *J. Environ. Radioact.* 192, 14–25. <https://doi.org/10.1016/j.jenvrad.2018.05.016>.
- Singh, S.K., Wang, M., Staudt, C., Iliakis, G., 2011. Post-irradiation chemical processing of DNA damage generates double-strand breaks in cells already engaged in repair. *Nucleic Acids Res.* 39 (19), 8416–8429. <https://doi.org/10.1093/nar/gkr463>.
- Song, Y., Asselman, J., De Schampelaere, K.A.C., Salbu, B., Tollefsen, K.E., 2018. Deciphering the combined effects of environmental stressors on gene transcription: a conceptual approach. *Environ. Sci. Technol.* 52 (9), 5479–5489. <https://doi.org/10.1021/acs.est.8b00749>.
- Song, Y., Rundberget, J.T., Evenseth, M.L., Xie, L., Gomes, T., Høgåsen, T., Iguchi, T., Tollefsen, K.E., 2016. Whole-organism transcriptomic analysis provides mechanistic insight into the acute toxicity of emamectin benzoate in daphnia magna. *Environ. Sci. Technol.* <https://doi.org/10.1021/acs.est.6b03456>.
- Sparks, E., Wachsman, G., Benfey, P.N., 2013. Spatiotemporal signalling in plant development. *Nat. Rev. Genet.* 14 (9), 631–644. <https://doi.org/10.1038/nrg3541>.
- Steffens, B., Sauter, M., 2005. Epidermal cell death in rice is regulated by ethylene, gibberellin, and abscisic acid. *Plant Physiol.* 139 (2), 713–721. <https://doi.org/10.1104/pp.105.064469>.
- Tang, X., Zhang, N., Si, H., Calderón-Urrea, A., 2017. Selection and validation of reference genes for RT-qPCR analysis in potato under abiotic stress. *Plant Methods* 13, 85. <https://doi.org/10.1186/s13007-017-0238-7>.
- Terada, H., 1990. Uncouplers of oxidative phosphorylation. *Environ. Health Perspect.* 87, 213–218. <https://doi.org/10.1289/ehp.9087213>.
- Teramura, A.H., Sullivan, J.H., 1994. Effects of UV-B radiation on photosynthesis and growth of terrestrial plants. *Photosynth. Res.* 39 (3), 463–473. <https://doi.org/10.1007/BF00014599>.
- Thorne, M.C., 2003. Background radiation: natural and man-made. *J. Radiol. Prot.* 23 (1), 29–42. <https://doi.org/10.1088/0952-4746/23/1/302>.
- UNSCEAR, 2021. Sources, Effects and Risks of Ionizing Radiation, United Nations Scientific Committee on the Effects of Atomic Radiation (UNSCEAR) 2019 Report. United Nations <https://doi.org/10.18356/9789210051361>.
- Van Hoeck, A., Horemans, N., Van Hees, M., Nauts, R., Knapen, D., Vandenhove, H., Blust, R., 2015. Characterizing dose response relationships: chronic gamma radiation in Lemna minor induces oxidative stress and altered polyploidy level. *J. Environ. Radioact.* 150, 195–202. <https://doi.org/10.1016/j.jenvrad.2015.08.017>.
- Vandesompele, J., De Preter, K., Pattyn, F., Poppe, B., Van Roy, N., De Paep, A., Speleman, F., 2002. Accurate normalization of real-time quantitative RT-PCR data by geometric averaging of multiple internal control genes. *Genome Biol.* 3 (7), Research0034. <https://doi.org/10.1186/gb-2002-3-7-research0034>.
- Vanhoudt, N., Horemans, N., Wannijn, J., Nauts, R., Van Hees, M., Vandenhove, H., 2014. Primary stress responses in Arabidopsis thaliana exposed to gamma radiation. *J. Environ. Radioact.* 129, 1–6. <https://doi.org/10.1016/j.jenvrad.2013.11.011>.
- Vu, C.V., Allen Jr., L.H., Garrard, L.A., 1981. Effects of supplemental UV-B radiation on growth and leaf photosynthetic reactions of soybean (*Glycine max*). *Physiol. Plant.* 52 (3), 353–362. <https://doi.org/10.1111/j.1399-3054.1981.tb06054.x>.
- Xie, L., Gomes, T., Solhaug, K.A., Song, Y., Tollefsen, K.E., 2018. Linking mode of action of the model respiratory and photosynthesis uncoupler 3,5-dichlorophenol to adverse outcomes in Lemna minor. *Aquat. Toxicol.* 197, 98–108. <https://doi.org/10.1016/j.aquatox.2018.02.005>.
- Xie, L., Solhaug, K.A., Song, Y., Brede, D.A., Lind, O.C., Salbu, B., Tollefsen, K.E., 2019. Modes of action and adverse effects of gamma radiation in an aquatic macrophyte Lemna minor. *Sci. Total Environ.* 680, 23–34. <https://doi.org/10.1016/j.scitotenv.2019.05.016>.
- Xie, L., Solhaug, K.A., Song, Y., Johnsen, B., Olsen, J.E., Tollefsen, K.E., 2020. Effects of artificial ultraviolet B radiation on the macrophyte Lemna minor: a conceptual study for toxicity pathway characterization. *Planta* 252 (5), 86. <https://doi.org/10.1007/s00425-020-03482-3>.